

Review

Computational Fluid Dynamics on Solar Dish in a Concentrated Solar Power: A Bibliometric Review

Aristotle T. Ubando ^{1,2,3,4,*} , Ariel Conversion ¹, Renyl B. Barroca ^{5,6} , Nelson H. Enano, Jr. ^{5,6} 
and Randell U. Espina ^{5,6} 

- ¹ Mechanical Engineering Department, De La Salle University, 2401 Taft Avenue, Manila 0922, Philippines; ariel_conversion@dlsu.edu.ph
 - ² National Research Council of the Philippines, Department of Science and Technology, 51 General Santos Avenue, Taguig City 1631, Philippines
 - ³ Thermomechanical Analysis Laboratory, De La Salle University–Laguna Campus, LTI Spine Road, Laguna Blvd, Biñan 4024, Philippines
 - ⁴ Center for Engineering and Sustainable Development Research, De La Salle University, 2401 Taft Avenue, Manila 0922, Philippines
 - ⁵ Center for Renewable Energy and Appropriate Technologies, Ateneo de Davao University, Davao City 8000, Philippines; rbarroca@addu.edu.ph (R.B.B.); nhenanojr@addu.edu.ph (N.H.E.J.); ruespina@addu.edu.ph (R.U.E.)
 - ⁶ Mindanao Renewable Energy R&D Center, Department of Science and Technology, Gen. Santos Avenue Bicutan, Taguig City 1631, Philippines
- * Correspondence: aristotle.ubando@dlsu.edu.ph



Citation: Ubando, A.T.; Conversion, A.; Barroca, R.B.; Enano, N.H., Jr.; Espina, R.U. Computational Fluid Dynamics on Solar Dish in a Concentrated Solar Power: A Bibliometric Review. *Solar* **2022**, *2*, 251–273. <https://doi.org/10.3390/solar2020014>

Academic Editors: Javier Muñoz Antón and Jürgen Heinz Werner

Received: 24 February 2022

Accepted: 26 April 2022

Published: 6 May 2022

Publisher's Note: MDPI stays neutral with regard to jurisdictional claims in published maps and institutional affiliations.



Copyright: © 2022 by the authors. Licensee MDPI, Basel, Switzerland. This article is an open access article distributed under the terms and conditions of the Creative Commons Attribution (CC BY) license (<https://creativecommons.org/licenses/by/4.0/>).

Abstract: Concentrated solar power is an alternative renewable energy technology that converts solar energy into electrical energy by using a solar concentrator and a solar receiver. Computational fluid dynamics have been used to numerically design concentrated solar power. This is a powerful numerical analysis approach that is widely used in energy and environmental engineering applications. In this paper, we review previous work on the applications of computational fluid dynamics in the design of concentrated solar power technology. We performed a bibliometric analysis of journal articles relevant to applications to analyze the current trend of utilization of computational fluid dynamics in these technologies. Then, we conducted a comprehensive analysis focused on the design of solar dish technology using computational fluid dynamics. Furthermore, we reviewed in detail the optical modeling of solar concentrators and solar receivers. Of the 83 retrieved publications from Scopus database, 80 were journal articles, and only three were review papers. Among these 80 journal articles, only 54 were relevant to this study, and 23 were relevant to solar dish technology. The documents were analyzed according to their number of citations, journal sources, and keyword evolution and network map. The information presented in this paper is useful to further recognize the contributions of computational fluid dynamics to the development of concentrated solar power, particularly to solar dish technology. In addition, we also discuss the challenges and future research directions to make solar energy a more sustainable source of renewable energy.

Keywords: computational fluid dynamics; concentrated solar power; solar dish; renewable energy; bibliometric analysis

1. Introduction

Concentrated solar power (CSP) is a promising technology for harnessing and utilizing a clean and sustainable source of energy. CSP consists of a solar concentrator that collects and intensifies the heat energy from the Sun and a solar receiver that converts the heat generated to produce electrical energy. Despite its recent adoption and the acceptance from both the scientific communities and energy investors, solar power still accounts for a very small percentage of total energy use [1]. The challenge in the optimal design of CSP is to make the technology more cost efficient and environmentally friendly. With the

advancement of numerical modeling software and computational hardware, most of the design problems in CSP technology have recently been solved using computational fluid dynamics (CFD).

Previous reviews have reported the application of CFD in the field of solar energy. Al-Abidi et al. [2] reviewed the various phase changing materials (PCMs) in solar photovoltaic (PV) ventilation and the application of CFD in the evaluation of its heat transfer behavior. Liu et al. [3] recently reviewed the different models and equations used to describe the PCM composites. Yadav and Bhagoria [4] conducted a review on the assessment of the heat transfer and the fluid flow of numerous solar air heaters using CFD. Solar air heater is a technology that converts solar energy into thermal energy and is usually integrated into solar PV panels. Kasaeian et al. [5] provided a comprehensive review of previous experimental, analytical, and simulation studies (which include the CFD approach) related to solar chimney applications. Moreover, Nadda et al. [6] presented a review of studies that investigate the application of jet impingement in increasing solar PV efficiency. The investigation approaches include experimental, CFD, and mathematical modeling. Chen et al. [7] published a bibliometric review on the development of concentrated solar power technologies but did not mention of any use of CFD modeling. Only a few reviews were found which discussed the application of CFD modeling in concentrated solar power technologies and focused on parabolic trough. As an example, Yilmaz and Mwesigye [8] performed a comprehensive review on several computational approaches that include CFD in the design of parabolic trough solar collectors. Olia et al. [9] and Bellos et al. [10] also presented a review on the application of nanofluids with CFD modeling in the enhancement of the thermal performance of parabolic trough technology. However, for solar dish technology with CFD modeling, no prior bibliometric review has yet been presented. No review studies were found to have evaluated the operating performance and analyzed the maximum thermal efficiency of the CSP for various types of receivers.

In this paper, we present a bibliometric review of the application of computational fluid dynamics in modeling concentrated solar power. The novelty of this work is that we evaluate the operating performance of various CSP technologies and compare the maximum thermal efficiency for different types of solar receivers. In addition, the bibliometric review highlights the evolution of keywords, the collaboration between authors, the most cited articles, and the top journal sources of publications related to CFD and CSP. The content analysis focuses only on the CFD modeling of solar dish technology, particularly on the concentrator and receiver side. The current challenges and future perspectives are also presented in this paper. Figure 1 shows the keyword network map for this topic generated using VosViewer. There are four main clusters of keywords, but the major keywords appearing are “computational fluid dynamics”, “solar energy”, and “concentrated solar power”.

1.1. Solar Energy

Solar energy is the most abundant renewable energy resource on Earth. Since one of the major problems today in the area of energy is finding an alternative source of clean and sustainable energy to replace fossil fuels, the focus of contemporary research has been on renewable energies, which include solar energy [11]. Solar energy is the only renewable energy source with enormous potential when compared to any level of human energy use [12].

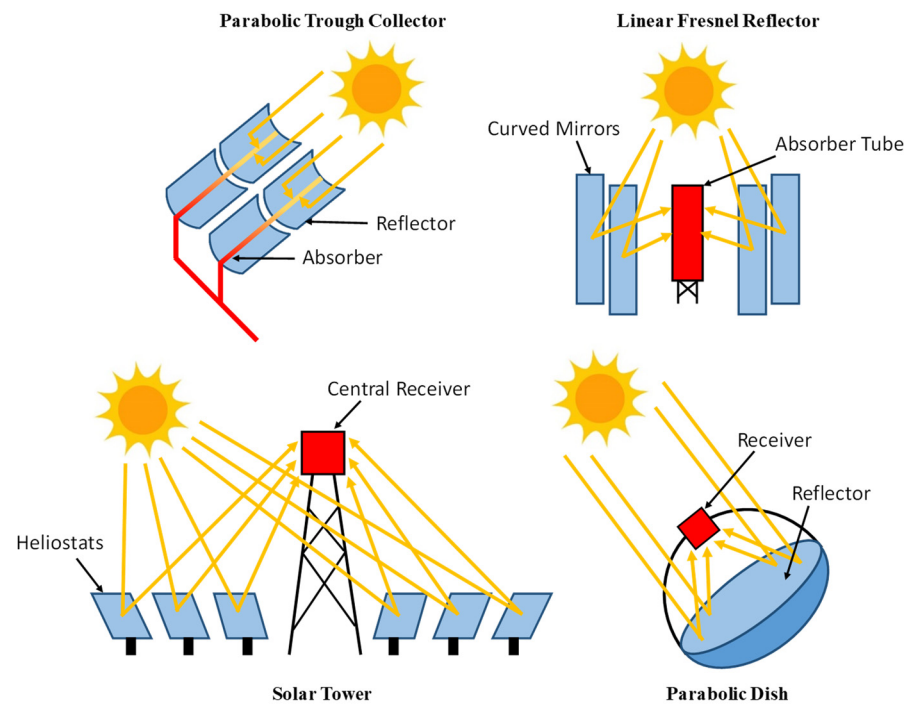


Figure 2. Concentrated solar power technologies.

1.3. Computational Fluid Dynamics

Computational fluid dynamics (CFD) is a powerful numerical analysis approach in solving various engineering and environment problems. It is a simulation technique that uses numerical equations and digital computers for iterative methods to model and to predict various heat, mass, and momentum transfer and fluid flow problems for the optimization of designs [4]. CFD is an accepted methodology by the scientific and engineering communities to design various types of renewable energy technologies [17]. There are three main stages of CFD study, as shown in Figure 3: pre-processing, processing, and post-processing. The pre-processing stage includes the geometry creation, the material assignment, mesh generation, and assignment of load and boundary conditions. After that, the governing equations such as the Navier–Stokes equation and the set of algorithms are computed and automatically processed by computers. Finally, the obtained results are visualized and interpreted during the post-processing stage.

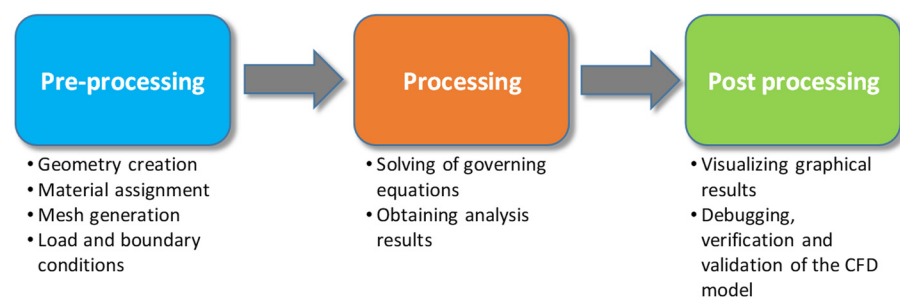


Figure 3. Computational fluid dynamics stages.

2. Bibliometric Analysis

2.1. Methodology

Figure 4 illustrates the methodological framework and research approach of this study. The data for published documents were obtained using the Scopus search keywords “computational fluid dynamics” OR “cfD” AND “concentrated solar power” OR “solar

dish" OR "parabolic dish". Originally, using only the keyword "computational fluid dynamics" OR "cfd" AND "concentrated solar power", the Scopus database provided only 66 documents as of 1 December 2020. To find other relevant documents, the keywords "solar dish" OR "parabolic dish" were added, which yielded a total of 83 documents. These yielded numbers were already refined by considering only articles and review documents. The information for the published papers was exported into a single csv file from Scopus. The downloaded csv file was then used as corpus for bibliometric analysis in CorText Manager. The CorText Manager was able to extract the important terms as well as the information from the corpus and to perform bibliometric analysis.

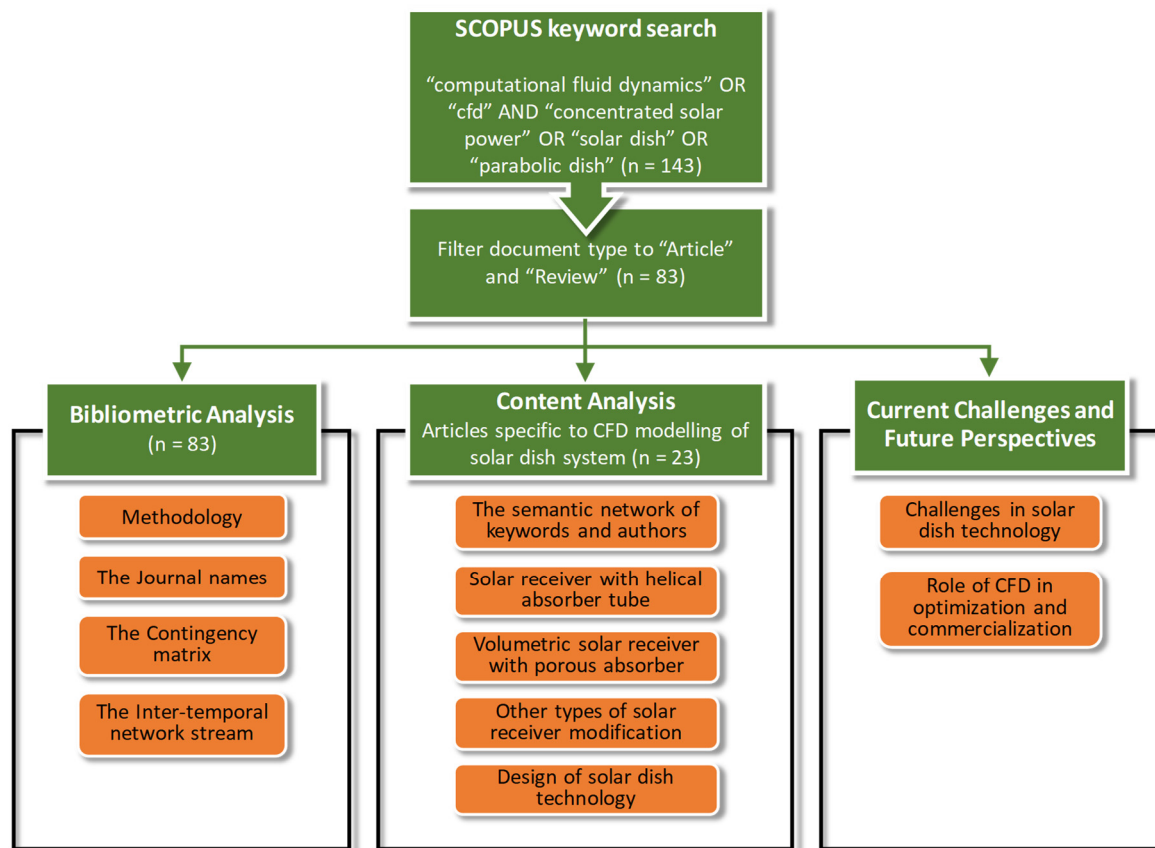


Figure 4. The methodological framework of the study.

2.2. The Journal Names

The extracted data from the Scopus database revealed that there are 30 different journal sources contributing to the study of "computational fluid dynamics modeling of concentrated solar power". Figure 5 shows the top ten most cited journals. It was found that the journal with the highest number of documents is *Solar Energy* with 24 published documents, followed by *Applied Energy* with 9 documents. However, the journal with the highest number of citations per publication is *Journal of Solar Energy Engineering, Transactions of the ASME*, followed by *Applied Energy*, with 65 and 49 citations per publication, respectively. The most cited journal articles are presented in Table 1. It shows that the most cited article is by [18].

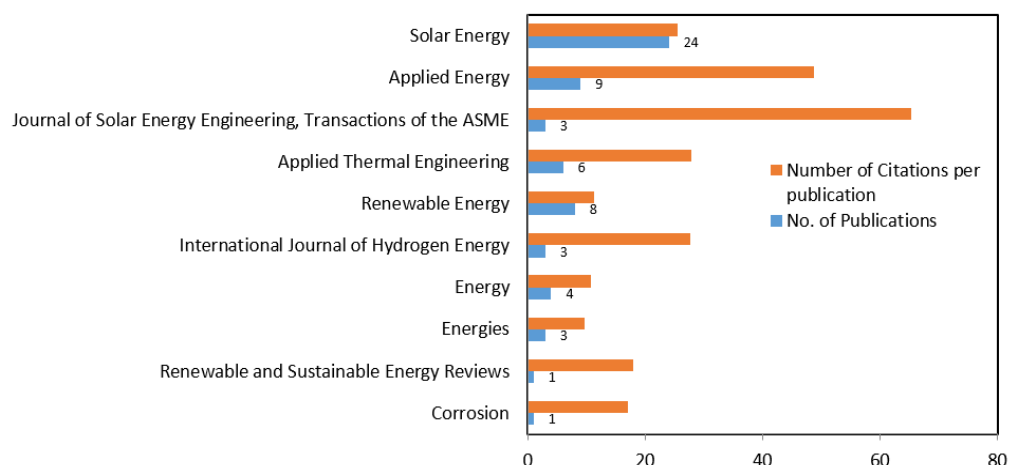


Figure 5. Top 10 journal sources with the highest number of citations.

Table 1. Top 5 most cited papers.

Author(s)	Title	Year	Cited by
Prakash M. et al. [18]	Investigations on heat losses from a solar cavity receiver	2009	160
Longeon M. et al. [11]	Experimental and numerical study of annular PCM storage in the presence of natural convection	2013	124
Taumoefolau T. et al. [19]	Experimental investigation of natural convection heat loss from a model solar concentrator cavity receiver	2004	123
Li Z. et al. [20]	Study on the radiation flux and temperature distributions of the concentrator-receiver system in a solar dish/Stirling power facility	2011	85
Yilmaz İ.H. and Mwesigye A. [8]	Modeling, simulation and performance analysis of parabolic trough solar collectors: A comprehensive review	2018	80

2.3. The Contingency Matrix

The terms from the published papers including the author's keyword, index keyword, and abstract words were extracted using the lexical term extraction algorithm in CorText Manager [21]. After the csv file from the Scopus database was uploaded as a corpus, the data were parsed and then the lexical term extraction algorithm of CorText Manager was able to list the top 100 terms, specifically noun phrases with at most three words each term. The listed terms were identified based on a minimum frequency of three co-occurrences in the csv file. The extracted terms were then used in generating the contingency matrix, as presented in Figure 6. The number of nodes selected was 10 for the sake of readability, with the extracted terms as the first field and the source titles (or the journal names) as the second field. The contingency matrix shows a heat map by which the colors of cells represent the degree of correlation between the two fields. Cells with red color mean a strong relationship between the two fields while the blue color means the opposite. In addition, the white color of the cell means that the two fields have no relationship [22]. For example, in Figure 6, the term "pressure drop" has a very strong connection to the journal *Energy*. In contrast, the term "natural convection" and the journal *Solar Energy* have a weak connection. Furthermore, the color gradient scale on the right side of the heat map indicates the deviation of the observed value of co-occurrences of the two fields from the expected value. For instance, if the cell value is 6, then the observed co-occurrence is 600% higher than the expected value. Conversely, if the cell has a value of -6 , the observed value of co-occurrence is 600% lower than expected. The basis for selecting the important terms is a chi-squared analysis measure, which is a statistical metric of co-occurrence and is widely used for analyzing significant biases between expected and observed frequencies [23]. Through this contingency matrix, the correlation between a specific term and a journal can be easily identified.

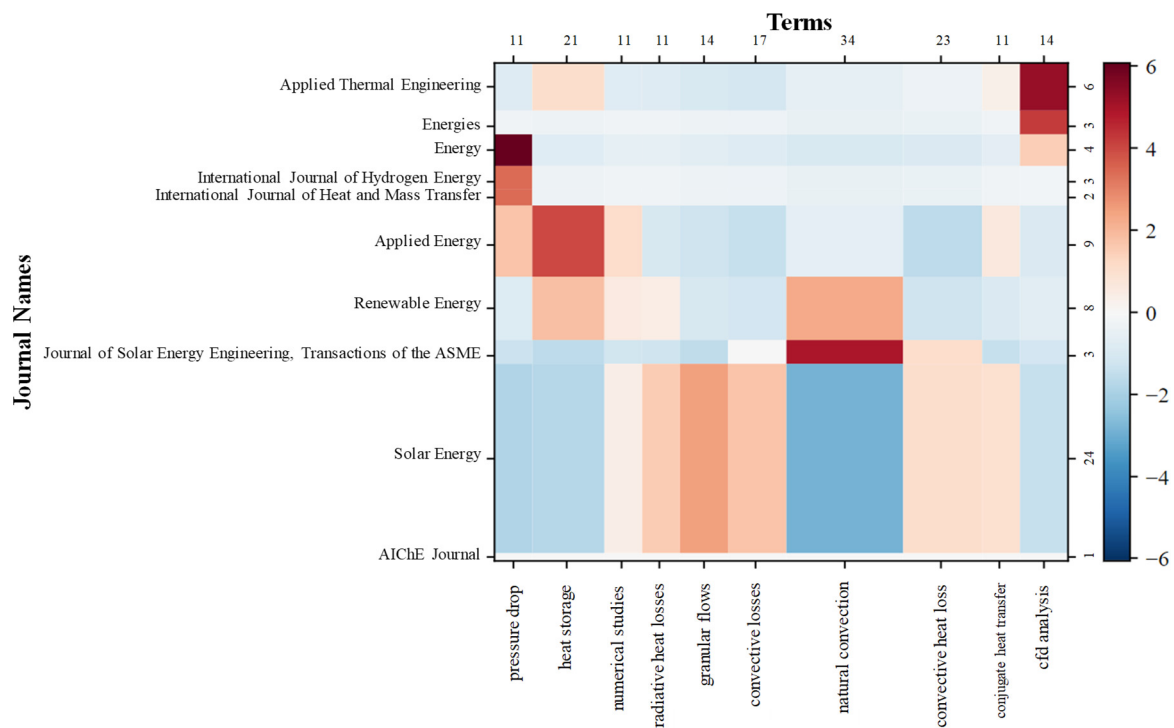


Figure 6. Contingency matrix of journals and keywords based on Scopus search keywords “computational fluid dynamics” and “concentrated solar power” or “solar dish” (1 December 2020).

2.4. The Inter-Temporal Network Stream

Using CorText Manager and with the same corpus as used in the contingency matrix, an inter-temporal network stream of the term to term is represented by a Sankey diagram in Figure 7. The terms were extracted from the csv file using the lexical term extraction algorithm, the same method used for the contingency matrix, and the diagram shows the transformation of terms over time in the form of streams. For the sake of readability and interpretability, the number of nodes was limited to 50 and the number of time slices was set to 3 with a homogenous distribution. In the figure, the width of tubes corresponds to the co-occurrence of the two terms. The terms “convective heat loss” and “radiation heat losses”, for instance, occur together more frequently in the published papers compared to the terms “radiative transfer equation” and “conjugate heat transfer”. The color of tubes represents the link strength of two terms. Tubes with darker colors mean that the two terms shared more nodes between two consecutive time periods [22].

From the Sankey diagram, it can be observed that the terms “radiative heat transfer” and “conjugate heat transfer” split into two separate streams (“ray effects and conjugate heat transfer” and “wind direction and linear Fresnel collector”) in the year 2016. It can also be observed that the terms “heat storage” and “thermal storage” and the terms “radiative transfer equation” and “conjugate heat transfer” converged into a single stream, “ray effects and conjugate heat transfer” in 2016. From 2016, this stream converged with the stream of “liquid metals and central receiver system” to form a single stream in 2020, the “wind speeds and inclination angles”. Through this Sankey diagram, the evolution and emergence of terms or keywords in the research area of CFD modeling of CSP can be analyzed.

The bump graph in Figure 8 was generated using CorText Manager, showing the evolution of the most mentioned terms in the topic of computational fluid dynamics modeling of concentrated solar power extracted using lexical term extraction algorithm. The size of the hierarchy was set to 4 and the number of time slices was 3 with a regular time slice distribution. It can be observed from the graph that even before 2005, the term “natural convection” had already been mentioned with an almost steady pattern until the present year. It can also be noted the increasing growth of the term “heat storage” over time.

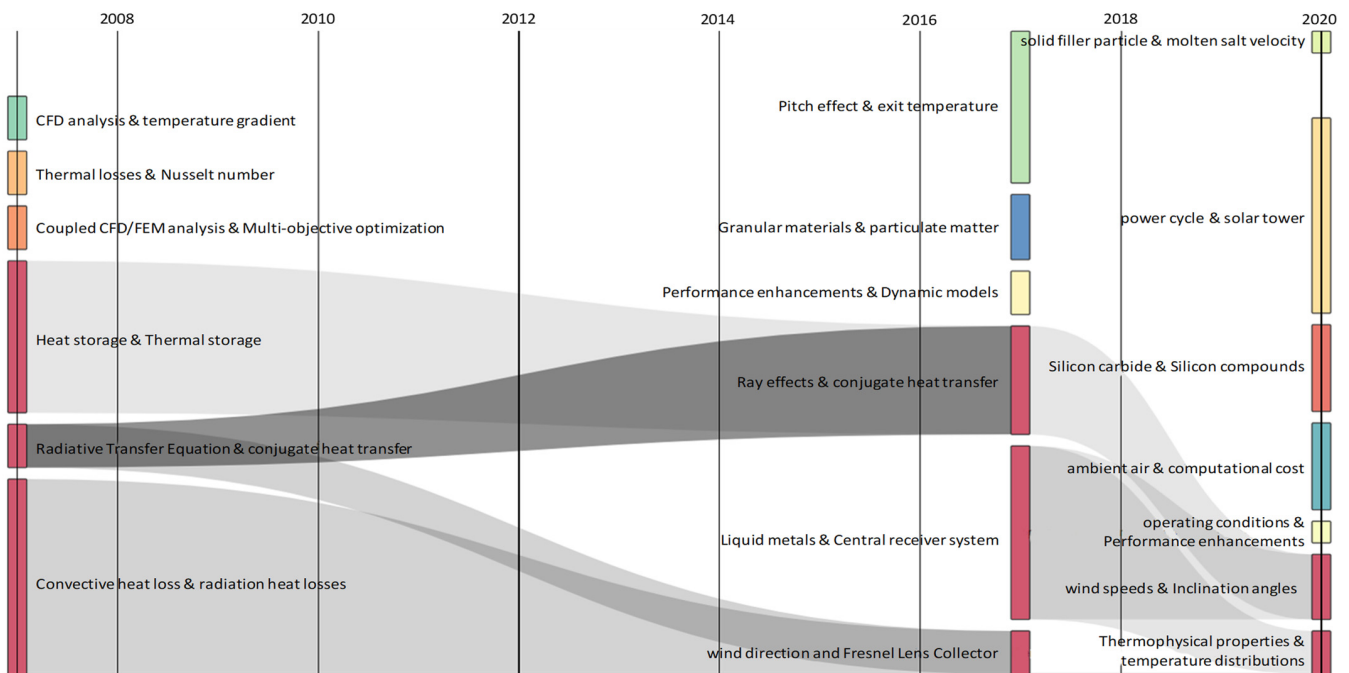


Figure 7. The Sankey diagram of keywords based on Scopus search keywords “computational fluid dynamics” and “concentrated solar power” or “solar dish” (1 December 2020).

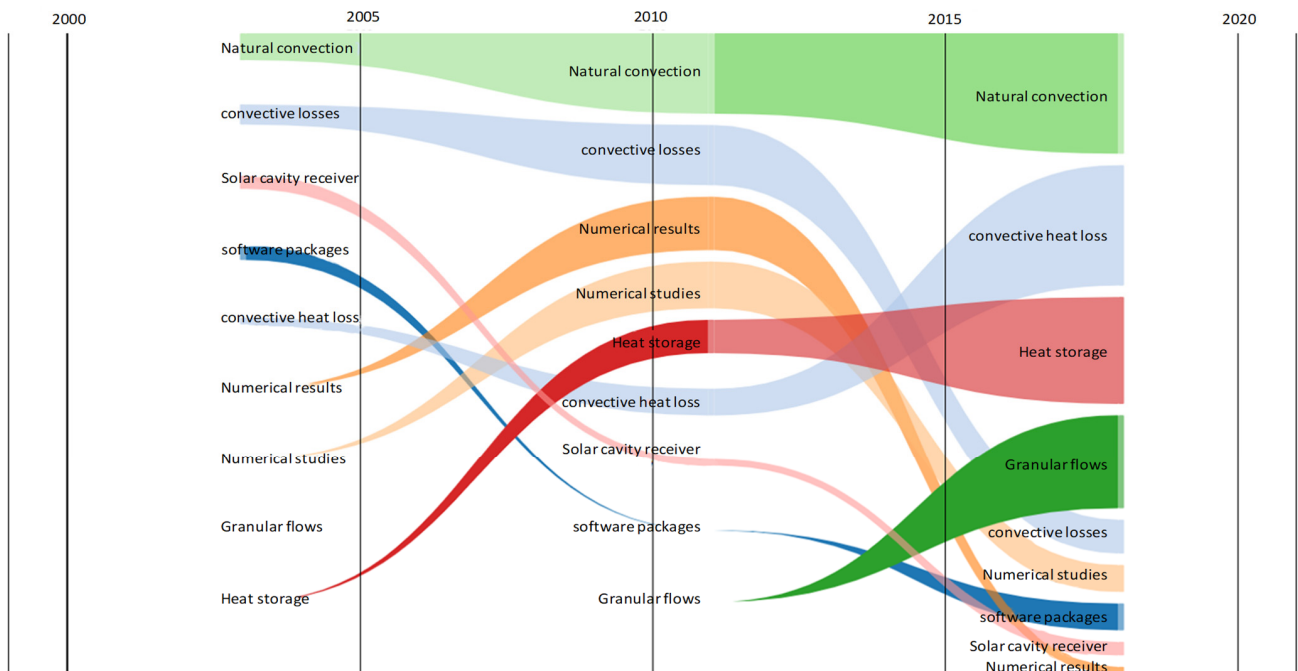


Figure 8. The bump graph of keywords based on Scopus search keywords “computational fluid dynamics” and “concentrated solar power” or “solar dish” (1 December 2020).

3. The CFD Modeling of Solar Dish System

3.1. The Semantic Network of Keywords and Authors

In this section, the contents of published journal articles relevant to the topic of computational fluid dynamics modeling of solar dish are analyzed. A review paper by Hachicha et al. [16] presented content analyses on the numerical models of the other types of CSP, which are central receiver or solar tower and parabolic through concentrator (PTC),

Table 2. Solar dish and receiver data.

References	Collector Size (mm)	Collector Reflectivity	Solar Irradiance (W/m ²)	Receiver Type	Receiver Size (mm)	Tube Size (mm)	Receiver Material
[24]	-	0.8	1000	rectangular with helical pipe	-	-	highly oxidized stainless steel at 1000 K
[25]	-	0.95	500–1000	cylindrical with helical tube	dr = 200, L = 300	dt = 8	steel with copper tube
[26]	-	0.95	800	cylindrical porous volumetric receiver	dr = 50, L = 50	3 (pore size)	open-cell SiC ceramic foam absorber
[27]	-	-	-	square porous absorber module	s = 10 × 10, L = 40	-	
[28]	D = 5060 * f = 3200	0.9	1000	conical with built-in helical pipe	dmax = 460 L = 170–630 Loop no. = 4–15	dt = 42	304 stainless steel (pipe and outer cover)
[29]	D = 1120 f = 700	0.95	800	cylindrical porous volumetric receiver	dr = 50, L = 50	3 (pore size)	open-cell SiC ceramic foam absorber
[30]	S = 1600 (square)	0.92	826	conical with helical tube	dmax = 38, L = 50	-	Inconel sheets coated with Pyromark 2500 paint
[31]	D = 2880 f = 1500	0.75	787	cylindrical with helically baffled cavity	dr = 200, L = 400	-	carbon steel
[32]	-	-	-	porous volumetric solar receiver	-	-	SiC ceramic foam absorber
[33]	-	-	-	cylinder with hollowed cylindrical cavity zoom with U-shaped air channel	dr = 290, L = 320	w × t = 68 × 4	
[34]	D = 200	0.737	800	porous volumetric solar receiver	-	4 (pore size) porosity = 85%	SiSiC open cell foam absorber
[35]	-	-	500	cylindrical container with 12 U-tubes	dr = 380, L = 440	dt = 15	Silicon Carbide (SiC)
[36]	D = 5000 f = 1840	-	-	conical	dr = 300, L = 710	-	
[37]	D = 1000	-	-	cylindrical, conical, and spherical with helical tube	dr = 200, L = 250 dr = 200, L = 354.3 dr = 200, L = 218	dt = 10	copper tube
[38]	D = 1000 to 5000	-	500–1000	cylindrical, conical, and spherical with helical tube	dr = 225, L = 235 dr = 225, L = 240 d r = 225, L = 257	dt = 19	copper tube
[39]	D = 1000 f = 455–555	0.95	525	cylindrical, conical, and spherical with helical tube	dr = 200, L = 250 dr = 200, L = 354.3 dr = 200, L = 218	dt = 20	copper tube
[40]	D = 3800 f = 2260	0.98	800	flat circular disk with spiral coil receiver	dmax = 404	dt = 9.3	
[41]	-	-	906	porous volumetric solar receiver	dr = 145.3	4 (cell diameter) 81.1% (porosity)	open-cell SiC ceramic foam absorber
[42]	-	-	-	cylindrical dish receiver	-	-	
[43]	f = 13,100 A = 425 m ²	-	-		-	-	
[20]	-	0.95	1000	shallow semi-ellipsoidal receiver, hemispherical, deep semi-ellipsoidal receiver	-	-	
[44]	-	-	-	hemispherical with spiral tubes			copper tube
[18]	-	-	-	cylindrical with helical tube	dr = 330, L = 500	dt = 9	copper tube coated with polyurethane

* D = aperture diameter; f = focus length; S = square aperture side; A = aperture area; dr = receiver diameter; dmax = maximum receiver diameter; dt = tube diameter; w × t = width and thickness; L = receiver height; s = side dimension.

Table 3 provides the data for the heat transfer fluid (which includes flow rate, inlet, and outlet fluid temperature) as well as the receiver efficiency (which includes the optical and thermal efficiency). Table 4 is a separate table for CFD and radiation models, listing the different CFD and optical simulation software used by the authors. Moreover, the other 48 articles which contain CFD modeling but are not specific to the solar dish are listed in Table 5 with their corresponding focus of CFD modeling. The rest, after assessment, are not relevant to CFD modeling.

Table 3. Heat transfer fluid and receiver efficiency.

References	Heat Transfer Fluid	Flow Rate (kg/s)	Inlet Fluid Temperature (°C)	Outlet Fluid Temperature (°C)	Max. Optical Efficiency (%)	Max. Thermal Efficiency (%)
[24]	air	0.06	657	679	70	50
[25]	air	0.009–0.02	24	70	-	-
[26]	air	-	27	334	-	80.6
[27]	air	-	25	700	-	-
[28]	air	0.03	350	-	87.6	72.7
[29]	air	-	27	475	93.7	85.5
[30]	water	0.0011	18.1	206	-	-
[31]	water	0.007–0.15	15–45	94.7	-	65
[32]	air	-	20	108.5	-	-
[33]	air	-	-	-	-	-
[34]	air	0.07	540	815	-	86.2 (receiver efficiency)
[35]	PCM (HTF) air (WF)	0.1 (air)	590	826	-	60 (receiver efficiency)
[37]	air	0.01	102	132.7 (cylindrical) 136.4 (conical) 128 (spherical)	-	-
[38]	air	0.01	102	131.2 (cylindrical) 134.8 (conical) 132.8 (spherical)	93	87
[39]	air	0.01	102	126.2 (cylindrical) 131 (conical) 124.2 (spherical)	91 (conical)	69 (cylindrical) 77.05 (conical) 63 (spherical)
[40]	-	-	-	-	95	-
[41]	air	0.147	568	780	-	86.7
[42]	air	-	-	-	-	-
[20]	-	-	-	-	-	60.7
[44]	air	-	-	-	-	-
[18]	water	0.02	50–75	-	-	-

Table 4. CFD and radiation models.

References	CFD Models	Radiation Models	Software Used for CFD	Software Used for Optics
[24]	-	-	Ansys Fluent	Soltrace
[25]	-	Surface to surface (S2S) radiation model	ANSYS Fluent	OptisWorks
[26]	-	MCRT method (for solar radiation transmission)	OpenFoam	Tonatiuh
[27]	-	-	ANSYS CFX	-
[28]	Boussinesq model k- ϵ turbulence model	MCRT S2S model	ANSYS 17.0	TracePro 7.3.4
[29]	finite volume method SIMPLE-for pressure-velocity coupling	MCRT P1 spherical harmonics method	OpenFoam	Octave 3.6.0
[30]	laminar model	-	ANSYS Fluent	-
[31]	k- ϵ turbulence model	MCRT S2S	ANSYS Fluent	SolTrace
[32]	SIMPLE algorithm	-	ANSYS Fluent 17.1	-

Table 4. *Cont.*

References	CFD Models	Radiation Models	Software Used for CFD	Software Used for Optics
[33]	SIMPLE to couple pressure-velocity fields based on FVM k- ϵ turbulence model	-	Fluent 17.0 and ICEM	-
[34]	-	MCRT	COMSOL	MATLAB based ray tracing calculation
[35]	solidification and melting model k- ϵ turbulence model	S2S	ANSYS Fluent 18.0	-
[36]	Shear Stress Transport (SST) turbulence model	-	ANSYS CFX 15.0.7	-
[37]	-	S2S	ANSYS	OptisWorks
[38]	-	MCRT	ANSYS Fluent	OptisWorks
[39]	k- ϵ turbulence model	MCRT S2S	ANSYS Fluent	OptisWorks
[40]	-	MCRT	-	TracePro
[41]	k- ϵ turbulence model	-	COMSOL Multiphysics	-
[42]	k- ϵ and k-kl- ω turbulence model	Discrete ordinates radiation model	ANSYS Fluent and SolidWorks Flow Simulation	-
[43]	SST k- ω turbulence model	-	ANSYS Fluent	-
[20]	FVM SIMPLEC (pressure-velocity coupling)	MCRT	FLUENT	TracePro
[44]	SIMPLEC (pressure-velocity coupling)	S2S	FLUENT	-
[18]	SIMPLEC (pressure-velocity coupling)	-	FLUENT	-

Table 5. The 48 documents that are relevant to CFD modeling of CSP-related technologies but not specific to solar dish technology.

Paper No.	Title	CFD Modeling Focus	References
1	Passive performance enhancement of parabolic trough solar concentrators using internal radiation heat shields	Parabolic trough	El-Bakry et al. [45]
2	Single-tank thermal energy storage systems for concentrated solar power: Flow distribution optimization for thermocline evolution management	Storage tank	Lou et al. [46]
3	Advancing Radiative Heat Transfer Modeling in High-Temperature Liquid Salts	Liquid salts	Coyle et al. [47]
4	The suitability of microscale compressed air axial turbine for domestic solar powered Brayton cycle	Turbine	Daabo et al. [48]
5	A comprehensive parametric study on integrated thermal and mechanical performances of molten-salt-based thermocline tank	Molten salt tank	Wang et al. [49]
6	Earth-cooling air tunnels for thermal power plants: Initial design by CFD modeling	Cooling system	de la Rocha Camba and Petrakopoulou [50]
7	Consistent coupled optical and thermal analysis of volumetric solar receivers with honeycomb absorbers	Solar tower	Ali et al. [51]
8	Evaluation of Thermophysical Properties of Menthol-Based Deep Eutectic Solvent as a Thermal Fluid: Forced Convection and Numerical Studies	Heat transfer fluid	Dehury et al. [52]

Table 5. Cont.

Paper No.	Title	CFD Modeling Focus	References
9	Computational fluid dynamics study to reduce heat losses at the receiver of a solar tower plant	Solar tower	Schmitt et al. [53]
10	A computational approach to simulate the optical and thermal performance of a novel complex geometry solar tower molten salt cavity receiver	Solar tower	Slootweg et al. [54]
11	Thermal-hydraulic performance of printed circuit heat exchangers with zigzag flow channels	Heat exchanger	Chen et al. [55]
12	An improved, generalized effective thermal conductivity method for rapid design of high temperature shell-and-tube latent heat thermal energy storage systems	Phase changing material (PCM)	Mostafavi Tehrani et al. [56]
13	Design and CFD analysis of an industrial low-pressure compressor for a concentrating high-temperature solar power plant	Compressor design	Cuturi et al. [57]
14	A study of granular flow through horizontal wire mesh screens for concentrated solar power particle heating receiver applications–Part II: Parametric model predictions	Solid particles in heat transfer medium	Sandlin and Abdel-Khalik [58]
15	An experimental and numerical study of granular flows through a perforated square lattice for central solar receiver applications	Solid particles in heat transfer medium	Sandlin and Abdel-Khalik [59]
16	Three-dimensional numerical simulation of upflow bubbling fluidized bed in opaque tube under high flux solar heating	Solar tower	Benoit et al. [60]
17	Wind barriers optimization for minimizing collector mirror soiling in a parabolic trough collector plant	Wind barriers	Moghimi and Ahmadi [61]
18	Geometry optimization of a heat storage system for concentrated solar power plants (CSP)	PCM heat storage system	Solé et al. [62]
19	Mixing enhancement in thermal energy storage molten salt tanks	Molten salt tank	Iranzo et al. [63]
20	Analysis of the performance of linear Fresnel collectors: Encapsulated vs. evacuated tubes	Fresnel lens	Cagnoli et al. [64]
21	Thermal energy storage for CSP hybrid gas turbine systems: Dynamic modeling and experimental validation	Thermal energy storage	Mahmood et al. [65]
22	Assessment of Heat Exchangers for the Integration of Concentrated Solar Energy into the Catalytic Hydrothermal Gasification of Biomass	Thermal energy storage	Viereck et al. [66]
23	Volume of fluid approach of boiling flows in concentrated solar plants	Fresnel Lens	Dinsenmeyer et al. [67]
24	Thermal cycle and combustion analysis of a solar-assisted micro gas turbine	Combustor side	Abagnale et al. [68]
25	Dense gas-particle suspension upward flow used as heat transfer fluid in solar receiver: PEPT experiments and 3D numerical simulations	Solar tower	Ansart et al. [69]
26	Optimized volumetric solar receiver: Thermal performance prediction and experimental validation	Volumetric solar receiver	Capuano et al. [70]

Table 5. Cont.

Paper No.	Title	CFD Modeling Focus	References
27	A comparison between transient CFD and FEM simulations of solar central receiver tubes using molten salt and liquid metals	Solar tower	Fritsch et al. [71]
28	Finite-volume ray tracing using Computational Fluid Dynamics in linear focus CSP applications	Fresnel lens	Craig et al. [72]
29	Coupled modeling of a directly heated tubular solar receiver for supercritical carbon dioxide Brayton cycle: Optical and thermal-fluid evaluation	Solar tower	Ortega et al. [73]
30	Recirculating metallic particles for the efficiency enhancement of concentrated solar receivers	Solar tower	Sarker et al. [74]
31	Aerodynamics of new solar parametric troughs: Two dimensional and three dimensional single module numerical analysis	Parabolic trough	Núñez Bootello et al. [75]
32	Dimensionless analysis for predicting Fe-Ni-Cr alloy corrosion in molten salt systems for concentrated solar power systems	Molten salt	Cho et al. [76]
33	CFD analysis of melting process in a shell-and-tube latent heat storage for concentrated solar power plants	PCM heat storage system	Fornarelli et al. [15]
34	Multidimensional modeling of nickel alloy corrosion inside high temperature molten salt systems	Corrosion in molten salt	Mehrabadi et al. [77]
35	Investigation of heat transfer enhancement in a new type heat exchanger using solar parabolic trough systems	Parabolic trough	Şahin et al. [78]
36	Optimization of a trapezoidal cavity absorber for the Linear Fresnel Reflector	Fresnel lens	Moghimi et al. [79]
37	A novel computational approach to combine the optical and thermal modeling of Linear Fresnel Collectors using the finite volume method	Fresnel lens	Moghimi et al. [80]
38	Assessment of a falling solid particle receiver with numerical simulation	Solar tower	Gobereit et al. [81]
39	Numerical simulation of particulate flow in interconnected porous media for central particle-heating receiver applications	Porous solar receiver	Lee et al. [82]
40	CFD-based reduced model for the simulation of thermocline thermal energy storage systems	Thermal energy storage	Pizzolato et al. [83]
41	CFD analysis of solar tower Hybrid Pressurized Air Receiver (HPAR) using a dual-banded radiation model	Solar tower	Craig et al. [84]
42	Thermal energy storages analysis for high temperature in air solar systems	Thermal energy storage	Andreozzi et al. [85]
43	Night time performance of a storage integrated solar thermophotovoltaic (SISTPV) system	Thermal energy storage (PV)	Veeraragavan et al. [86]
44	Numerical study of wind forces on parabolic solar collectors	Parabolic trough	Zemler et al. [87]
45	CFD-simulation of a new receiver design for a molten salt solar power tower	Solar tower	Garbrecht et al. [88]

Table 5. Cont.

Paper No.	Title	CFD Modeling Focus	References
46	Modular object-oriented methodology for the resolution of molten salt storage tanks for CSP plants	Molten salt tank	Rodríguez et al. [14]
47	Experimental and numerical study of annular PCM storage in the presence of natural convection	PCM heat storage tank	Longeon et al. [11]
48	Numerical study of conduction and convection heat losses from a half-insulated air-filled annulus of the receiver of a parabolic trough collector	Parabolic trough	Al-Ansary and Zeitoun [89]

3.2. Solar Receiver with Helical Absorber Tube

A solar receiver with a helical tube as an absorber is the most common type of receiver configuration used in the studies, accounting for 9 out of 23 articles relevant to CFD modeling of solar dish systems. Prakash et al. [18] performed a CFD simulation using Fluent to estimate the convective heat losses in a cylindrical receiver with skirt. The inlet temperature (from 50 °C to 300 °C) was varied as well as the receiver inclination angle (0°, 30°, 45°, 60°, and 90°). The results of numerical study were compared to the experimental data and yielded a maximum deviation of about 14%. Also using Fluent and SolidWorks Flow simulation software, Yuan et al. [42] were able to predict the convective heat losses for two different solar receiver models, which were cubical cavity and cylindrical cavity receiver. The simulation results were compared against the experimental data and showed that the simulation result for the cylindrical receiver model was in good agreement with the experimental result. The effect of different turbulence and air property model options in Fluent were also analyzed and compared. Daabo et al. [39] focused on evaluating the optical efficiency and heat flux distribution of cylindrical-, conical-, and spherical-shaped solar receivers. The absorption ratio of each geometric configuration was measured and showed that conical-shaped geometry has the highest value. The optimal distance of focal location of the cavity receiver was also determined using OptisWorks software and the CFD simulation was carried out by Fluent and then validated by experimental results of published works. Daabo et al. [38] adapted the OptisWorks software based on the Monte Carlo Ray Tracing (MCRT) method and CFD software ANSYS Fluent to examine the optical and thermal performance of the same type of receiver used previously. The optical simulation result of irradiance absorbed by the receiver was used as an input parameter to the CFD analysis using User Define Function (UDF) to simulate the flow and heat transfer performance of the working fluid while varying some parameters such as reflector diameter and coil pitch of the helical tube. It was observed from the results that a zero-coil pitch has better performance than a 0.5 D pitch. It was added that the overall system performance can be enhanced when the receiver is covered by glass.

Then, Daabo et al. [37] studied the effect of coil pitch and tube diameter on the working fluid's exit temperature and found that the conical-shaped receiver was more efficient than the other two geometries tested. Meanwhile, Uzair et al. [36] studied the influence of wind flow on the heat loss from the receiver while varying the orientation of the solar dish concentrator employing computational fluid dynamics in ANSYS CFX. The heat loss analysis was different from most studies which focused on the heat loss due to natural convection. The results showed that the dish orientation indeed significantly affects the flow structure near the receiver, which consequently contributes to heat loss.

Zhang et al. [28] performed combined optical and thermal numerical modeling to optimize the performance of a solar conical receiver with a built-in helical pipe. The simulation was able to obtain the optimal values of conical angle, loop number, and insulation thickness to maximize the optical and thermal efficiency of the cavity receiver using TracePro optics software and ANSYS CFD software, which were also compared to published experimental data. Then, Daabo et al. [90] presented an optical and thermal

simulations of a micro-scale cylindrical cavity receiver for the Brayton gas power cycle while varying the solar radiation. The flux distribution in the receiver cavity was predicted using OptisWorks software, and the obtained data became the basis for determining the energy absorbed by the compressed air as HTF through CFD simulation in ANSYS. The results, which were validated through experiments, showed the best configurations of the cavity receiver which can be used for domestic applications of concentrated solar power. Moreover, Craig et al. [24] employed the combined CFD and ray-tracing software in estimating the heat losses of a tubular cavity dish receiver at various inclination angles. The heat source profile was obtained using the Monte Carlo ray tracing method in SolTrace software and was used as input in ANSYS Fluent through user-defined functions. It was concluded and validated through previous literature that the thermal efficiency was mainly affected by the convective heat losses.

3.3. Volumetric Solar Receiver with Porous Absorber

Another type of solar receiver configuration is the volumetric solar receiver with a porous media as the absorber. Based on the extracted data from Scopus, the first published article regarding CFD modeling of a volumetric solar receiver in a solar dish system was in 2015. Aichmayer et al. [41] designed a small-scale solar concentrator using a porous volumetric absorber in the solar receiver integrated with a hybrid micro-gas turbine system with considerations of system efficiency, pressure drop, material utilization, and economic cost. The initial detailed analysis of the results was performed using a coupled CFD/FEM tool in COMSOL Multiphysics. It was found that the use of a volumetric receiver in a solar dish system is a promising technology in harnessing solar energy. Aichmayer et al. [34] utilized CFD/FEM in COMSOL software routines for the thermo-mechanical analysis of the OMSoP solar dish system using a porous receiver and coupled to a MATLAB-based ray tracing routine for a heat source calculation. The numerical simulations were performed to verify the results of the presented systematic scaling methodology for the solar dish system using a KTH high-flux solar simulator before selecting a suitable receiver configuration for full-scale application. Then, Zhao et al. [32] employed CFD simulation to investigate and verify the results of coupled a multiple-relaxation-time lattice Boltzmann model (MRT-LBM) of flow and heat transfer performance of a porous volumetric receiver. Three types of porous structures have been developed and studied, and the influence of some parameters such as pore structure, Reynolds number, and thermal diffusivity of solid matrix were presented. In addition, Barreto et al. [29] used three-dimensional modeling based on the finite volume method (FVM) in OpenFOAM (an open source software) to analyze the thermal performance of cylindrical porous volumetric receivers made of open-cell SiC ceramic foam absorber. The propagation and absorption of solar radiation was developed in Octave software using the Monte Carlo ray tracing (MCRT) method which was then coupled to CFD. Different assumptions were applied such as the adiabatic boundary to obtain a detailed analysis of the temperature profiles near the wall. With this assumption in place, it was found that the most accurate results were obtained when the heat flux separation was applied between the solid and fluid located at the side wall. Moreover, Barreto et al. [26] conducted a detailed CFD simulation using OpenFOAM for cylindrical porous volumetric receiver with open-cell silicon carbide (SiC) ceramic foam as the absorber. Tonatiuh software was utilized for ray-tracing from the parabolic dish to the receiver. A parametric analysis was performed to determine the optimal values of porosity, pore size, and inlet velocity. Meanwhile, Herrmann et al. [27] formulated a CFD model in ANSYS CFX to verify the proposed assimilation framework using blower actuation in addressing the current challenges in open volumetric solar receivers. Challenges presented included the fluctuation in the intensity of radiation flux which may sometimes produce thermal shocks and unexpected thermal loads on the porous ceramic absorber. The proposed solution was able to resolve the problems in the volumetric solar receiver by stabilizing the flow temperature gradients.

3.4. Other Types of Solar Receiver Modification

There are other types of solar receiver modifications that do not belong to either of the two categories. Kumar and Reddy [44] performed a numerical study based on asymptotic computational fluid dynamics (ACFD) in estimating the convective and radiation heat loss from a hemispherical receiver with spiral tubes while varying the inclination angles from 0° to 90° inclination. The influences of emissivity, temperature ratio, and diameter ratio on heat loss were also investigated. Li et al. [20] used TracePro ray-tracing software based on the Monte Carlo ray tracing method to numerically simulate the radiation flux profiles in a solar receiver tested in three different types of configurations: shallow semi-ellipsoidal, hemispherical, and deep semi-ellipsoidal receiver. The obtained flux profile was then used as a boundary condition for CFD simulation to analyze the heat transfer fluid's behavior in the cavity receiver of the Stirling power system. The numerical modeling results were validated through an experiment using Xe-arc lamps as a heat source. Christo [43] presented numerical calculations of velocity and pressure fields, and dust particle trajectories of a hexagonal parabolic dish using ANSYS Fluent. The wind speeds were varied and the flow field structure as well as the lift and drag coefficients were obtained while varying the dish orientations. The study provided a good assessment of how to effectively reduce the aerodynamics drag of the solar dish structure. Pavlović et al. [40] performed a numerical simulation using TracePro software from Lambda Research, USA, to compare the optical performance of a flat circular disk and corrugated coil receiver, both having a spiral absorber. The optimal position and diameter of the receiver were also investigated and it was presented in the results that the optimal position was 2.075 m from the reflector surface, which is lower than the focal point of the reflector, and the optimal diameter of the receiver was found to be 400 mm. Another receiver modification was developed by Giovannelli and Bashir [35], which was a solar receiver made of a cylindrical container with 12 U-tubes and submerged in a Phase Change Material (PCM) which acts as a short-term storage system. The charge and discharge behavior of the PCM were analyzed using ANSYS Fluent CFD and the results showed that the proposed concept of short-term storage system has a potential application in solar dish micro gas turbine (MGT) systems since it was able to maintain the temperature in the working fluid for 20–30 min.

Yang et al. [33] proposed a forced airflow concept in reducing the convective heat loss in the solar dish receiver. The geometry considered was a hallowed cylindrical cavity zoom with a U-shaped air channel and modeled in Fluent and ICEM software for CFD calculation. There were also two types of air circulation mode compared, the clockwise and anticlockwise circulation, and the results showed that the system can be improved better using the anticlockwise mode. Soltani et al. [31] studied the optical and thermal performance of a helically baffled cylindrical cavity receiver both theoretically and experimentally. First, an optical simulation was conducted for solar flux distribution in the collector and receiver using SolTrace MCRT software to minimize the computational cost before proceeding to the thermal simulation of real flux distribution in ANSYS Fluent. The combined optical and thermal simulation increased the accuracy of the numerical simulation, and the results showed a good agreement with the experimental data with a maximum deviation of only about 2%. The results also concluded that the receiver aperture distance from the focal point of the concentrator has a significant effect on the thermal performance of the CSP system. Lastly, Khalil et al. [30] presented a three-dimensional CFD laminar model using ANSYS Fluent to predict the fluid flow and heat transfer behavior of a thermo-plate conical cavity receiver made of welded sheets of 0.5 mm Inconel-625 with pressurized water as the heat transfer fluid (HTF) and a serpentine fluid path. Since the Reynolds number exceeded the laminar flow domain, it was planned to test the flow field using a turbulent model.

3.5. Design of Solar Dish Technology

We observed in the published studies regarding computational fluid dynamics modeling of solar dish systems that there are two main types of solar receivers, the receiver with a helical tube absorber and the volumetric solar (VSR) receiver with a porous absorber.

However, there are also other receiver modifications used for solar dish systems other than the two mentioned. For receivers with helical absorbers, the commonly used geometry configurations were cylindrical, conical, and spherical, but among these three, the conical shape was the most efficient type of receiver cavity, with an average thermal efficiency of 78.92%, and the rectangular cavity was the least efficient, with only 50% efficiency as provided in the literature. The data show that the thermal efficiency of receivers with helical tube absorbers varies largely depending on the shape of the receiver cavity. For the VSR, it was observed that the commonly used material for the absorber was made up of open-cell silicon carbide (SiC) ceramic foam. Between these two main types of solar receiver, the volumetric solar receiver with porous absorber was more efficient compared to the tubular receiver, as presented in Figure 10. It is shown in the figure that the thermal efficiencies of VSR with a porous absorber from four different studies were observed to be consistently higher, with an average value of 84.74%, relative to the thermal efficiencies of the receiver with helical absorber tube, with only 69.79% average thermal efficiency. This is due to the capability of the VSR to operate at relatively elevated temperatures [91,92]. In addition, the optimization on the geometry of the VSR by finding the optimal porosity and pore sizes of the absorber further enhances its thermal efficiency [26,41,44]. The other types of receivers with an average thermal efficiency of 61.9%, despite the modifications of the receiver design, were still less thermally efficient compared to the already established receiver designs such as the helical tube and the porous absorber.

The largest solar dish collector ever modeled in CFD was by Zhang et al. [29], which has an aperture diameter of 5.06 m. It was also noted from the articles that the optimal distance of the receiver cavity from the collector aperture is not necessarily the focal distance of the parabolic collector. Moreover, an optical modeling using the Monte Carlo ray tracing method for the radiation flux distribution was usually performed first before proceeding to the actual radiation model using CFD. The most popular CFD software for this topic is ANSYS Fluent, while for the optics simulation, it is the OptisWorks software.

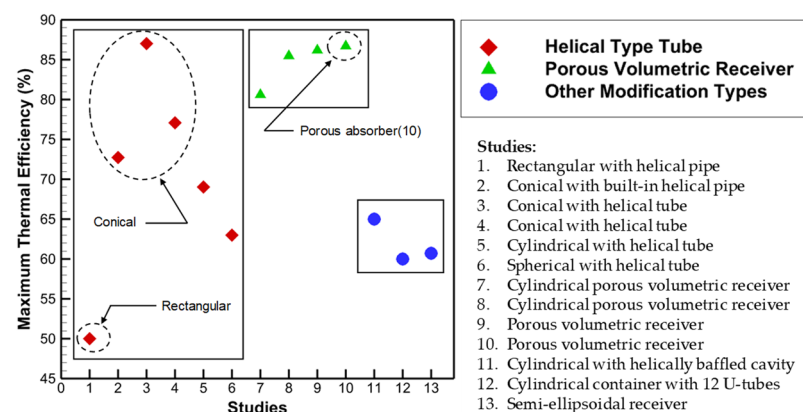


Figure 10. The maximum thermal efficiency of different types of solar dish receiver: (1) Craig et al. [24], (2) Zhang et al. [28], (3) Daabo et al. [38], (4–6) Daabo et al. [39], (7) Barreto et al. [26], (8) Barreto et al. [29], (9) Aichmayer et al. [34], (10) Aichmayer et al. [41], (11) Soltani et al. [31], (12) Giovannelli & Bashir [35], (13) Li et al. [20].

4. Current Challenges and Future Perspectives

Despite the accelerated development in concentrated solar power technologies, they are still facing many challenges. One of the current challenges in CSP technologies, particularly in solar dish technology, is finding the optimal configuration of the porous absorber in the volumetric solar receiver (VSR) which will increase not just the receiver efficiency but also its durability. A volumetric receiver with a porous receiver is the most promising type of solar receiver based on the value of efficiencies presented in Table 3 and Figure 10. In addition, this type of receiver is not only used in solar dish technology but also widely used

in solar tower receivers [51,70]. Hence, finding the optimal pore size and porosity as well as the material selection are among the concerns in the area of concentrated solar power. Moreover, another challenge in solar dish technology is the convective heat losses in the receiver. Craig et al. [24] addressed that the convective heat losses significantly affect the thermal efficiency of the CSP system and were even greater when the effect of wind speed surrounding the solar receiver was considered. Another great challenge is to integrate the use of phase changing material (PCM) in the solar dish system to stabilize the radiation flux in the receiver in a cloudy sky.

For the challenges in employing numerical analysis in solar dish systems, one major concern is to find the optimal distance of the receiver from the concentrator. This can be determined through an optical simulation since the focal distance of the concentrator is not always the optimal distance between the concentrator and the receiver. However, Zhang et al. [28] encountered a problem where a compromise between the optical efficiency and thermal efficiency was observed. It was highlighted that the decrease in optical efficiency increases the thermal efficiency of the receiver, which may affect the overall efficiency of the system. It is to be noted that the overall efficiency of a solar dish is a product of the optical and thermal efficiency. In addition, increasing the outlet fluid temperature does not always translate to an increase in thermal efficiency since the temperature of the receiver's internal walls also increases, which consequently increases the thermal losses [31]. Hence, there should be a detailed study on the combined optical and CFD simulation since the two approaches are performed using separate software.

The combined computational simulation of optical and CFD plays an important role in the enhancement of the design of the CSP, which leads to commercialization. With the combined simulation, a considerable reduction in capital cost of the CSP projects will be realized. In the design phase, the optimal sizes of equipment with respect to the performance and durability can be determined through computational simulations such as optical and CFD simulations.

5. Conclusions

We performed a bibliometric analysis of previous works on computational fluid dynamics on concentrated solar power technologies. The results revealed that there are 83 published documents relevant to the topic extracted from the Scopus database (as of 1 December 2020). In order to manage the analysis of data from Scopus, CorText Manager was employed to analyze the corpus. The keywords and important terms in abstracts were extracted using a lexical term extraction algorithm, and then the contingency matrix between the terms and journal names, the term-to-term Sankey diagram, the bump graph of keywords, and the network map of keywords and authors were presented. The results of the content analysis have shown that the most used type of solar receiver in solar dish systems is the helical tube absorber. However, the volumetric solar receivers with porous absorbers were found to be relatively more efficient compared to tubular receivers, with an average maximum thermal efficiency of 84.74%. The insights outlined in this study provide future perspectives on the application of computational fluid dynamics in the development of the solar dish technology.

Author Contributions: Conceptualization, A.T.U., R.B.B., N.H.E.J. and R.U.E.; methodology, A.T.U., A.C.; software, A.T.U., A.C.; validation, A.T.U., R.B.B. and A.C.; formal analysis, R.B.B., N.H.E.J. and R.U.E.; investigation, A.T.U. and A.C.; resources, A.T.U., R.B.B., N.H.E.J. and R.U.E.; data curation, A.T.U. and A.C.; writing—original draft preparation, A.C.; writing—review and editing, A.T.U., R.B.B., N.H.E.J. and R.U.E.; visualization, A.T.U. and A.C.; supervision, A.T.U.; project administration, A.T.U.; funding acquisition, A.T.U., R.B.B., N.H.E.J. and R.U.E. All authors have read and agreed to the published version of the manuscript.

Funding: This research received no external funding.

Institutional Review Board Statement: Not applicable.

Informed Consent Statement: Not applicable.

Data Availability Statement: All data used are available in publicly accessible repository.

Acknowledgments: The RDLEAD program of the Philippines' Department of Science and Technology under the Science for Change Program is gratefully acknowledged for the support of this work.

Conflicts of Interest: The authors declare no conflict of interest.

References

- Phillips, L. 9—Solar energy. In *Managing Global Warming*; Letcher, T.M., Ed.; Academic Press: Cambridge, MA, USA, 2019; pp. 317–332.
- Al-Abidi, A.A.; Bin Mat, S.; Sopian, K.; Sulaiman, M.Y.; Mohammed, A.T. CFD applications for latent heat thermal energy storage: A review. *Renew. Sustain. Energy Rev.* **2013**, *20*, 353–363. [[CrossRef](#)]
- Liu, M.; Sun, Y.; Bruno, F. A review of numerical modelling of high-temperature phase change material composites for solar thermal energy storage. *J. Energy Storage* **2020**, *29*, 101378. [[CrossRef](#)]
- Yadav, A.S.; Bhagoria, J.L. Heat transfer and fluid flow analysis of solar air heater: A review of CFD approach. *Renew. Sustain. Energy Rev.* **2013**, *23*, 60–79. [[CrossRef](#)]
- Kasaeian, A.B.; Molana, S.; Rahmani, K.; Wen, D. A review on solar chimney systems. *Renew. Sustain. Energy Rev.* **2017**, *67*, 954–987. [[CrossRef](#)]
- Nadda, R.; Kumar, A.; Maithani, R. Efficiency improvement of solar photovoltaic/solar air collectors by using impingement jets: A review. *Renew. Sustain. Energy Rev.* **2018**, *93*, 331–353. [[CrossRef](#)]
- Chen, Q.; Wang, Y.; Zhang, J.; Wang, Z. The knowledge mapping of concentrating solar power development based on literature analysis technology. *Energies* **2020**, *13*, 1988. [[CrossRef](#)]
- Yılmaz, İ.H.; Mwesigye, A. Modeling, simulation and performance analysis of parabolic trough solar collectors: A comprehensive review. *Appl. Energy* **2018**, *225*, 135–174. [[CrossRef](#)]
- Olia, H.; Torabi, M.; Bahiraei, M.; Ahmadi, M.H.; Goodarzi, M.; Safaei, M.R. Application of nanofluids in thermal performance enhancement of parabolic trough solar collector: State-of-the-art. *Appl. Sci.* **2019**, *9*, 463. [[CrossRef](#)]
- Bellos, E.; Tzivanidis, C.; Tsimpoukis, D. Enhancing the performance of parabolic trough collectors using nanofluids and turbulators. *Renew. Sustain. Energy Rev.* **2018**, *91*, 358–375. [[CrossRef](#)]
- Longeon, M.; Soupart, A.; Fourmigué, J.F.; Bruch, A.; Marty, P. Experimental and numerical study of annular PCM storage in the presence of natural convection. *Appl. Energy* **2013**, *112*, 175–184. [[CrossRef](#)]
- Moriarty, P.; Honnery, D. 6—Global renewable energy resources and use in 2050. In *Managing Global Warming*; Letcher, T.M., Ed.; Academic Press: Cambridge, MA, USA, 2019; pp. 221–235.
- Junginger, M.; Louwen, A. Chapter 1—Introduction. In *Technological Learning in the Transition to a Low-Carbon Energy System*; Junginger, M., Louwen, A., Eds.; Academic Press: Cambridge, MA, USA, 2020; pp. 3–7.
- Rodríguez, I.; Pérez-Segarra, C.D.; Lehmkuhl, O.; Oliva, A. Modular object-oriented methodology for the resolution of molten salt storage tanks for CSP plants. *Appl. Energy* **2013**, *109*, 402–414. [[CrossRef](#)]
- Fornarelli, F.; Camporeale, S.M.; Fortunato, B.; Torresi, M.; Oresta, P.; Magliocchetti, L.; Miliozzi, A.; Santo, G. CFD analysis of melting process in a shell-and-tube latent heat storage for concentrated solar power plants. *Appl. Energy* **2016**, *164*, 711–722. [[CrossRef](#)]
- Hachicha, A.A.; Yousef, B.A.A.; Said, Z.; Rodríguez, I. A review study on the modeling of high-temperature solar thermal collector systems. *Renew. Sustain. Energy Rev.* **2019**, *112*, 280–298. [[CrossRef](#)]
- Ubando, A.T.; San, R.; Cruz, J.D.P. Savonius Wind Turbine Numerical Parametric Analysis Using Space-Filling Design and Gaussian Stochastic Process. *Wind* **2022**, *2*, 7. [[CrossRef](#)]
- Prakash, M.; Kedare, S.B.; Nayak, J.K. Investigations on heat losses from a solar cavity receiver. *Sol. Energy* **2009**, *83*, 157–170. [[CrossRef](#)]
- Taumoefolau, T.; Paitoonsurikarn, S.; Hughes, G.; Lovegrove, K. Experimental investigation of natural convection heat loss from a model solar concentrator cavity receiver. *J. Sol. Energy Eng. Trans. ASME* **2004**, *126*, 801–807. [[CrossRef](#)]
- Li, Z.; Tang, D.; Du, J.; Li, T. Study on the radiation flux and temperature distributions of the concentrator-receiver system in a solar dish/Stirling power facility. *Appl. Therm. Eng.* **2011**, *31*, 1780–1789. [[CrossRef](#)]
- Ubando, A.T.; Africa, A.D.M.; Maniquiz-Redillas, M.C.; Culaba, A.B.; Chen, W.H.; Chang, J.S. Microalgal biosorption of heavy metals: A comprehensive bibliometric review. *J. Hazard. Mater.* **2021**, *402*, 123431. [[CrossRef](#)]
- Marvuglia, A.; Havinga, L.; Heidrich, O.; Fonseca, J.; Gaitani, N.; Reckien, D. Advances and challenges in assessing urban sustainability: An advanced bibliometric review. *Renew. Sustain. Energy Rev.* **2020**, *124*, 109788. [[CrossRef](#)]
- Matsuo, Y.; Ishizuka, M. Key word extraction from a document using word co-occurrence statistical information. *Trans. Jpn. Soc. Artif. Intell.* **2002**, *17*, 217–223. [[CrossRef](#)]
- Craig, K.J.; Slootweg, M.; Le Roux, W.G.; Wolff, T.M.; Meyer, J.P. Using CFD and ray tracing to estimate the heat losses of a tubular cavity dish receiver for different inclination angles. *Sol. Energy* **2020**, *211*, 1137–1158. [[CrossRef](#)]

25. Daabo, A.M.; Bellos, E.; Pavlovic, S.; Bashir, M.A.; Mahmoud, S.; Al-Dadah, R.K. Characterization of a micro thermal cavity receiver—Experimental and analytical investigation. *Therm. Sci. Eng. Prog.* **2020**, *18*, 100554. [[CrossRef](#)]
26. Barreto, G.; Canhoto, P.; Collares-Pereira, M. Parametric analysis and optimisation of porous volumetric solar receivers made of open-cell SiC ceramic foam. *Energy* **2020**, *200*, 117476. [[CrossRef](#)]
27. Herrmann, B.; Behzad, M.; Cardemil, J.M.; Calderón-Muñoz, W.R.; Fernández, R.M. Conjugate heat transfer model for feedback control and state estimation in a volumetric solar receiver. *Sol. Energy* **2020**, *198*, 343–354. [[CrossRef](#)]
28. Zhang, Y.; Xiao, H.; Zou, C.; Falcoz, Q.; Neveu, P. Combined optics and heat transfer numerical model of a solar conical receiver with built-in helical pipe. *Energy* **2020**, *193*, 116775. [[CrossRef](#)]
29. Barreto, G.; Canhoto, P.; Collares-Pereira, M. Three-dimensional CFD modelling and thermal performance analysis of porous volumetric receivers coupled to solar concentration systems. *Appl. Energy* **2019**, *252*, 113433. [[CrossRef](#)]
30. Khalil, I.; Pratt, Q.; Spittle, C.; Codd, D. Modeling a thermoplate conical heat exchanger in a point focus solar thermal collector. *Int. J. Heat Mass Transf.* **2019**, *130*, 1–8. [[CrossRef](#)]
31. Soltani, S.; Bonyadi, M.; Madadi Avargani, V. A novel optical-thermal modeling of a parabolic dish collector with a helically baffled cylindrical cavity receiver. *Energy* **2019**, *168*, 88–98. [[CrossRef](#)]
32. Zhao, W.; Zhang, Y.; Xu, B.; Li, P.; Wang, Z.; Jiang, S. Multiple-relaxation-time lattice Boltzmann simulation of flow and heat transfer in porous volumetric solar receivers. *J. Energy Resour. Technol. Trans. ASME* **2018**, *140*, 082003. [[CrossRef](#)]
33. Yang, S.; Wang, J.; Lund, P.D.; Wang, S.; Jiang, C. Reducing convective heat losses in solar dish cavity receivers through a modified air-curtain system. *Sol. Energy* **2018**, *166*, 50–58. [[CrossRef](#)]
34. Aichmayer, L.; Garrido, J.; Laumert, B. Scaling effects of a novel solar receiver for a micro gas-turbine based solar dish system. *Sol. Energy* **2018**, *162*, 248–264. [[CrossRef](#)]
35. Giovannelli, A.; Bashir, M.A. Charge and discharge analyses of a PCM storage system integrated in a high-temperature solar receiver. *Energies* **2017**, *10*, 1943. [[CrossRef](#)]
36. Uzair, M.; Anderson, T.N.; Nates, R.J. The impact of the parabolic dish concentrator on the wind induced heat loss from its receiver. *Sol. Energy* **2017**, *151*, 95–101. [[CrossRef](#)]
37. Daabo, A.M.; Mahmoud, S.; Al-Dadah, R.K.; Ahmad, A. Numerical investigation of pitch value on thermal performance of solar receiver for solar powered Brayton cycle application. *Energy* **2017**, *119*, 523–539. [[CrossRef](#)]
38. Daabo, A.M.; Ahmad, A.; Mahmoud, S.; Al-Dadah, R.K. Parametric analysis of small scale cavity receiver with optimum shape for solar powered closed Brayton cycle applications. *Appl. Therm. Eng.* **2017**, *122*, 626–641. [[CrossRef](#)]
39. Daabo, A.M.; Mahmoud, S.; Al-Dadah, R.K. The optical efficiency of three different geometries of a small scale cavity receiver for concentrated solar applications. *Appl. Energy* **2016**, *179*, 1081–1096. [[CrossRef](#)]
40. Pavlović, S.R.; Vasiljević, D.M.; Stefanović, V.P.; Stamenković, Z.M.; Bellos, E.A. Optical analysis and performance evaluation of a solar parabolic dish concentrator. *Therm. Sci.* **2016**, *20*, S1237–S1249. [[CrossRef](#)]
41. Aichmayer, L.; Spelling, J.; Laumert, B. Preliminary design and analysis of a novel solar receiver for a micro gas-turbine based solar dish system. *Sol. Energy* **2015**, *114*, 378–396. [[CrossRef](#)]
42. Yuan, J.K.; Ho, C.K.; Christian, J.M. Numerical simulation of natural convection in solar cavity receivers. *J. Sol. Energy Eng. Trans. ASME* **2015**, *137*, 031004. [[CrossRef](#)]
43. Christo, F.C. Numerical modelling of wind and dust patterns around a full-scale paraboloidal solar dish. *Renew. Energy* **2012**, *39*, 356–366. [[CrossRef](#)]
44. Christo, F.C. Numerical modelling of wind Kumar, N.S.; Reddy, K.S. Investigation of convection and radiation heat losses from modified cavity receiver of solar parabolic dish using asymptotic computational fluid dynamics. *Heat Transf. Eng.* **2010**, *31*, 597–607. [[CrossRef](#)]
45. El-Bakry, M.M.; Kassem, M.A.; Hassan, M.A. Passive performance enhancement of parabolic trough solar concentrators using internal radiation heat shields. *Renew. Energy* **2021**, *165*, 52–66. [[CrossRef](#)]
46. Lou, W.; Fan, Y.; Luo, L. Single-tank thermal energy storage systems for concentrated solar power: Flow distribution optimization for thermocline evolution management. *J. Energy Storage* **2020**, *32*, 101749. [[CrossRef](#)]
47. Coyle, C.; Baglietto, E.; Forsberg, C. Advancing Radiative Heat Transfer Modeling in High-Temperature Liquid Salts. *Nucl. Sci. Eng.* **2020**, *194*, 782–792. [[CrossRef](#)]
48. Daabo, A.; Kreshat, Z.; Farhat, R.; Rahawi, K.; Mahmood, A.; Lattimore, T. The suitability of microscale compressed air axial turbine for domestic solar powered Brayton cycle. *Int. J. Energy Environ. Eng.* **2020**, *11*, 351–366. [[CrossRef](#)]
49. Wang, G.; Yu, S.; Niu, S.; Chen, Z.; Hu, P. A comprehensive parametric study on integrated thermal and mechanical performances of molten-salt-based thermocline tank. *Appl. Therm. Eng.* **2020**, *170*, 115010. [[CrossRef](#)]
50. de la Rocha Camba, E.; Petrakopoulou, F. Earth-cooling air tunnels for thermal power plants: Initial design by CFD modelling. *Energies* **2020**, *13*, 797. [[CrossRef](#)]
51. Ali, M.; Rady, M.; Attia, M.A.A.; Ewais, E.M.M. Consistent coupled optical and thermal analysis of volumetric solar receivers with honeycomb absorbers. *Renew. Energy* **2020**, *145*, 1849–1861. [[CrossRef](#)]
52. Dehury, P.; Chaudhary, R.K.; Banerjee, T.; Dalal, A. Evaluation of Thermophysical Properties of Menthol-Based Deep Eutectic Solvent as a Thermal Fluid: Forced Convection and Numerical Studies. *Ind. Eng. Chem. Res.* **2019**, *58*, 20125–20133. [[CrossRef](#)]
53. Schmitt, A.; Dinter, F.; Reichel, C. Computational fluid dynamics study to reduce heat losses at the receiver of a solar tower plant. *Sol. Energy* **2019**, *190*, 286–300. [[CrossRef](#)]

54. Slootweg, M.; Craig, K.J.; Meyer, J.P. A computational approach to simulate the optical and thermal performance of a novel complex geometry solar tower molten salt cavity receiver. *Sol. Energy* **2019**, *187*, 13–29. [[CrossRef](#)]
55. Chen, M.; Sun, X.; Christensen, R.N. Thermal-hydraulic performance of printed circuit heat exchangers with zigzag flow channels. *Int. J. Heat Mass Transf.* **2019**, *130*, 356–367. [[CrossRef](#)]
56. Mostafavi Tehrani, S.S.; Shoraka, Y.; Diarce, G.; Taylor, R.A. An improved, generalized effective thermal conductivity method for rapid design of high temperature shell-and-tube latent heat thermal energy storage systems. *Renew. Energy* **2019**, *132*, 694–708. [[CrossRef](#)]
57. Cuturi, N.; Aronica, S.; Bellini, L.; Salvati, A. Design and CFD analysis of an industrial low-pressure compressor for a concentrating high-temperature solar power plant. *Int. J. Thermodyn.* **2019**, *22*, 184–191. [[CrossRef](#)]
58. Sandlin, M.; Abdel-Khalik, S.I. A study of granular flow through horizontal wire mesh screens for concentrated solar power particle heating receiver applications—Part II: Parametric model predictions. *Sol. Energy* **2018**, *174*, 1252–1262. [[CrossRef](#)]
59. Sandlin, M.; Abdel-Khalik, S.I. An experimental and numerical study of granular flows through a perforated square lattice for central solar receiver applications. *Sol. Energy* **2018**, *174*, 463–473. [[CrossRef](#)]
60. Benoit, H.; Ansart, R.; Neau, H.; Garcia Triñanes, P.; Flamant, G.; Simonin, O. Three-dimensional numerical simulation of upflow bubbling fluidized bed in opaque tube under high flux solar heating. *AIChE J.* **2018**, *64*, 3857–3867. [[CrossRef](#)]
61. Moghimi, M.A.; Ahmadi, G. Wind barriers optimization for minimizing collector mirror soiling in a parabolic trough collector plant. *Appl. Energy* **2018**, *225*, 413–423. [[CrossRef](#)]
62. Solé, A.; Falcoz, Q.; Cabeza, L.F.; Neveu, P. Geometry optimization of a heat storage system for concentrated solar power plants (CSP). *Renew. Energy* **2018**, *123*, 227. [[CrossRef](#)]
63. Iranzo, A.; Suárez, C.; Guerra, J. Mixing enhancement in thermal energy storage molten salt tanks. *Energy Convers. Manag.* **2018**, *168*, 320–328. [[CrossRef](#)]
64. Cagnoli, M.; Mazzei, D.; Procopio, M.; Russo, V.; Savoldi, L.; Zanino, R. Analysis of the performance of linear Fresnel collectors: Encapsulated vs. evacuated tubes. *Sol. Energy* **2018**, *164*, 119–138. [[CrossRef](#)]
65. Mahmood, M.; Traverso, A.; Traverso, A.N.; Massardo, A.F.; Marsano, D.; Cravero, C. Thermal energy storage for CSP hybrid gas turbine systems: Dynamic modelling and experimental validation. *Appl. Energy* **2018**, *212*, 1240–1251. [[CrossRef](#)]
66. Viereck, S.; Keller, J.; Haselbacher, A.; Jovanovic, Z.R.; Steinfeld, A. Assessment of Heat Exchangers for the Integration of Concentrated Solar Energy into the Catalytic Hydrothermal Gasification of Biomass. *Energy Technol.* **2017**, *5*, 2086–2099. [[CrossRef](#)]
67. Dinsenmeyer, R.; Fourmigué, J.F.; Caney, N.; Marty, P. Volume of fluid approach of boiling flows in concentrated solar plants. *Int. J. Heat Fluid Flow* **2017**, *65*, 177–191. [[CrossRef](#)]
68. Abagnale, C.; Cameretti, M.C.; De Robbio, R.; Tuccillo, R. Thermal cycle and combustion analysis of a solar-assisted micro gas turbine. *Energies* **2017**, *10*, 773. [[CrossRef](#)]
69. Ansart, R.; García-Triñanes, P.; Boissière, B.; Benoit, H.; Seville, J.P.K.; Simonin, O. Dense gas-particle suspension upward flow used as heat transfer fluid in solar receiver: PEPT experiments and 3D numerical simulations. *Powder Technol.* **2017**, *307*, 25–36. [[CrossRef](#)]
70. Capuano, R.; Fend, T.; Stadler, H.; Hoffschmidt, B.; Pitz-Paal, R. Optimized volumetric solar receiver: Thermal performance prediction and experimental validation. *Renew. Energy* **2017**, *114*, 556–566. [[CrossRef](#)]
71. Fritsch, A.; Uhlig, R.; Marocco, L.; Frantz, C.; Flesch, R.; Hoffschmidt, B. A comparison between transient CFD and FEM simulations of solar central receiver tubes using molten salt and liquid metals. *Sol. Energy* **2017**, *155*, 259–266. [[CrossRef](#)]
72. Craig, K.J.; Moghimi, M.A.; Rungasamy, A.E.; Marsberg, J.; Meyer, J.P. Finite-volume ray tracing using Computational Fluid Dynamics in linear focus CSP applications. *Appl. Energy* **2016**, *183*, 241–256. [[CrossRef](#)]
73. Ortega, J.; Khivisara, S.; Christian, J.; Ho, C.; Yellowhair, J.; Dutta, P. Coupled modeling of a directly heated tubular solar receiver for supercritical carbon dioxide Brayton cycle: Optical and thermal-fluid evaluation. *Appl. Therm. Eng.* **2016**, *109*, 970–978. [[CrossRef](#)]
74. Sarker, M.R.I.; Saha, M.; Rahman, M.S.; Beg, R.A. Recirculating metallic particles for the efficiency enhancement of concentrated solar receivers. *Renew. Energy* **2016**, *96*, 850–862. [[CrossRef](#)]
75. Núñez Bootello, J.P.; Mier-Torrecilla, M.; Doblaré, M.; Silva Pérez, M. Aerodynamics of new solar parametric troughs: Two dimensional and three dimensional single module numerical analysis. *Sol. Energy* **2016**, *135*, 742–749. [[CrossRef](#)]
76. Cho, H.S.; Van Zee, J.W.; Shimpalee, S.; Tavakoli, B.A.; Weidner, J.W.; Garcia-Diaz, B.L.; Martinez-Rodriguez, M.J.; Olson, L.; Gray, J. Dimensionless analysis for predicting Fe-Ni-Cr alloy corrosion in molten salt systems for concentrated solar power systems. *Corrosion* **2016**, *72*, 742–760. [[CrossRef](#)]
77. Mehrabadi, B.A.T.; Weidner, J.W.; Garcia-Diaz, B.; Martinez-Rodriguez, M.; Olson, L.; Shimpalee, S. Multidimensional modeling of nickel alloy corrosion inside high temperature molten salt systems. *J. Electrochem. Soc.* **2016**, *163*, C830–C838. [[CrossRef](#)]
78. Şahin, H.M.; Baysal, E.; Dal, A.R.; Şahin, N. Investigation of heat transfer enhancement in a new type heat exchanger using solar parabolic trough systems. *Int. J. Hydrogen Energy* **2015**, *40*, 15254–15266. [[CrossRef](#)]
79. Moghimi, M.A.; Craig, K.J.; Meyer, J.P. Optimization of a trapezoidal cavity absorber for the Linear Fresnel Reflector. *Sol. Energy* **2015**, *119*, 343–361. [[CrossRef](#)]
80. Moghimi, M.A.; Craig, K.J.; Meyer, J.P. A novel computational approach to combine the optical and thermal modelling of Linear Fresnel Collectors using the finite volume method. *Sol. Energy* **2015**, *116*, 407–427. [[CrossRef](#)]

81. Gobereit, B.; Amsbeck, L.; Buck, R.; Pitz-Paal, R.; Röger, M.; Müller-Steinhagen, H. Assessment of a falling solid particle receiver with numerical simulation. *Sol. Energy* **2015**, *115*, 505–517. [[CrossRef](#)]
82. Lee, T.; Lim, S.; Shin, S.; Sadowski, D.L.; Abdel-Khalik, S.I.; Jeter, S.M.; Al-Ansary, H. Numerical simulation of particulate flow in interconnected porous media for central particle-heating receiver applications. *Sol. Energy* **2015**, *113*, 14–24. [[CrossRef](#)]
83. Pizzolato, A.; Donato, F.; Verda, V.; Santarelli, M. CFD-based reduced model for the simulation of thermocline thermal energy storage systems. *Appl. Therm. Eng.* **2015**, *76*, 391–399. [[CrossRef](#)]
84. Craig, K.J.; Gauché, P.; Kretzschmar, H. CFD analysis of solar tower Hybrid Pressurized Air Receiver (HPAR) using a dual-banded radiation model. *Sol. Energy* **2014**, *110*, 338–355. [[CrossRef](#)]
85. Andreozzi, A.; Buonomo, B.; Manca, O.; Tamburrino, S. Thermal energy storages analysis for high temperature in air solar systems. *Appl. Therm. Eng.* **2014**, *71*, 130–141. [[CrossRef](#)]
86. Veeraragavan, A.; Montgomery, L.; Datas, A. Night time performance of a storage integrated solar thermophotovoltaic (SISTPV) system. *Sol. Energy* **2014**, *108*, 377–389. [[CrossRef](#)]
87. Zemler, M.K.; Bohl, G.; Rios, O.; Boetcher, S.K.S. Numerical study of wind forces on parabolic solar collectors. *Renew. Energy* **2013**, *60*, 498–505. [[CrossRef](#)]
88. Garbrecht, O.; Al-Sibai, F.; Kneer, R.; Wiegardt, K. CFD-simulation of a new receiver design for a molten salt solar power tower. *Sol. Energy* **2013**, *90*, 94–106. [[CrossRef](#)]
89. Al-Ansary, H.; Zeitoun, O. Numerical study of conduction and convection heat losses from a half-insulated air-filled annulus of the receiver of a parabolic trough collector. *Sol. Energy* **2011**, *85*, 3036–3045. [[CrossRef](#)]
90. Bashir, M.A.; Daabo, A.M.; Amber, K.P.; Khan, M.S.; Arshad, A.; Elahi, H. Effect of phase change materials on the short-term thermal storage in the solar receiver of dish-micro gas turbine systems: A numerical analysis. *Appl. Therm. Eng.* **2021**, *195*, 117179. [[CrossRef](#)]
91. Fend, T.; Hoffschmidt, B.; Pitz-Paal, R.; Reutter, O.; Rietbrock, P. Porous materials as open volumetric solar receivers: Experimental determination of thermophysical and heat transfer properties. *Energy* **2004**, *29*, 823–833. [[CrossRef](#)]
92. Ho, C.K.; Iverson, B.D. Review of high-temperature central receiver designs for concentrating solar power. *Renew. Sustain. Energy Rev.* **2014**, *29*, 835–846. [[CrossRef](#)]